IR Fingerprints of U(VI) Nitrate Monoamides Complexes: A Joint Experimental and Theoretical Study

ARTICLE *in* THE JOURNAL OF PHYSICAL CHEMISTRY A · OCTOBER 2010

Impact Factor: 2.69 · DOI: 10.1021/jp106467p · Source: PubMed

8 AUTHORS, INCLUDING:

Antonio Prestianni
Università degli Studi di Palermo
24 PUBLICATIONS **352** CITATIONS
SEE PROFILE

L. Joubert
Université de Rouen
82 PUBLICATIONS **1,082** CITATIONS
SEE PROFILE

Alexandre Chagnes
Chimie ParisTech
64 PUBLICATIONS **685** CITATIONS
SEE PROFILE

Gerard Cote
École nationale supérieure de chimie de P…
154 PUBLICATIONS **2,077** CITATIONS
SEE PROFILE

IR Fingerprints of U(VI) Nitrate Monoamides Complexes: A Joint Experimental and Theoretical Study

Antonio Prestianni,[†] Laurent Joubert,[†] Alexandre Chagnes,[†] Gerard Cote,[†] Marie-Noelle Ohnet,[‡] Catherine Rabbe,[‡] Marie-Christine Charbonnel,[‡] and Carlo Adamo*,[†]

Laboratoire d'Electrochimie, Chimie des Interface et Modélisation pour l'Energie (UMR 7575), Ecole Nationale Supérieure de Chimie de Paris (Chimie Paristech), 11 rue Pierre et Marie Curie, F-75231 Paris Cedex 05, France, and Nuclear Energy Division, Radio Chemistry & Processes Department, Service of Chemistry in Separation Processes, Laboratory of Interactions Ligand-Actinide, CEA Marcoule, F-30207 Bagnols-sur-Cèze, France

Received: July 13, 2010; Revised Manuscript Received: August 24, 2010

Infrared spectra of 0.5 mol·L^{-1} uranium(VI) nitrate monoamide complexes in toluene have been recorded and compared with infrared spectra calculated by DFT. The investigated monoamides were *N*,*N*-dimethylformamide (DMF), *N*,*N*-dibutylformamide (DBF), and *N*,*N*-dicyclohexylformamide (DcHF). The validity of DFT calculations for describing uranium nitrate monoamide complexes has been confirmed as a fair agreement between experimental and calculated spectra was obtained. Furthermore, a topological analysis of the electron density has been carried out to characterize monoamide−uranium interactions. From this work, it appears that the increase of stability of uranylmonoamide complexes may be directly linked to the degree of polarization of the ligands in interaction with uranylnitrate. Among the investigated monoamides, the most stable complex is $UO_2(NO_3)_2$·2DcHF. This complex is characterized by a high positive charge delocalization in the outer part of the ligand molecule, which leads to a more concentrated positive charge close to the uranyl cation (UO_2^{2+}), thus strengthening the electrostatic interaction between the metal and the ligand.

1. Introduction

Liquid−liquid extraction is one of the most important separation processes in hydrometallurgy or nuclear fuel processing.[1,2] The performance of such processes relies mainly on the choice of adequate extractant molecules, which must gather specific chemical criteria, such as high extraction capacity, selectivity toward target metal species, low cost, resistance against chemical, and radiolysis stresses.[2] Nuclear solvent extraction processes implemented in the back-end and the front-end of the nuclear fuel cycle need to adapt constantly to different contraints, including environment regulation, new specifications, and composition of the feed solution. For instance, the PUREX (Plutonium Uranium Refining by EXtraction) process, implemented among others at Areva's La Hague plant for the reprocessing of nuclear spent fuel, uses tri-*n*-butyl phosphate (TBP) diluted to 30% in weight in tetrapropylen hydrogen (TPH).[3] This molecule permits selective extraction of uranium from concentrated nitric acid with a recovery yield of almost 99.9%.[3] Nevertheless, numerous studies concern the search of new extractants in order to increase the extraction ability and the selectivity in the frame of actinide partitioning. An important feature in this ligand design is the sturdiness against radiolytical degradation and its intrinsic composition (avoiding the use of organophosphorus molecules to reduce the bulk of secondary nuclear wastes).

N,*N*-Dialkylamides have been proposed as alternative to TBP for the reprocessing of nuclear fuel since 1960.[4] In fact, this class of ligands offers many advantages over organophosphorus compounds regarding their complete incinerability and the nature of radiolysis products easily removed by washing the degradated solvent. Numerous extraction studies have been performed, mainly focused on the applied aspects such as distribution coefficients of classical cations such as U(VI), Pu(IV), or Th(IV) and the degradation products and their impact.[5−7]

The nature of alkyl chains (R and R′) has influence on the affinity and selectivity of amides (such as RCONR′R′), as shown for example by the distribution ratio ranging from $D_{U(VI)} = 0.6$ with *N*,*N*-dibutylpivalamide to $D_{U(VI)} = 14$ with *N*,*N*-dicyclohexylacetamide under the same chemical conditions (0.5 mol L^{-1} monoamide diluted in toluene; nitric acid 3 M).[4,8]

There is thus a strong need, due to the major interest of both fundamental aspects of the rare earth coordination chemistry and of the design of new ligands with improved properties, to carry out more advanced studies. Today, fundamental studies on the molecular scale of such chemical systems remain sparse.[8−12] A better description of the bond between the amide group and the metal ion is a prerequisite to understand the relationship between the nature of the ligand and the affinity toward actinides in liquid−liquid conditions. One of the experimental techniques which can provide such information is the infrared spectroscopy. The main frequencies of interest for uranium−monoamide compounds are the $\nu_{C=O}$ and ν_{C-N} stretching frequencies but also the ν_{U-O} in the case of uranium amide complexes. However, vibrational spectra of amides and amide−cation complexes in solution are quite difficult to attribute due to the low molecular symmetry, which induces strong coupling among vibrational modes, and then, the complete assignment is quite difficult even for simple amides as dimethyl formamide (DMF).[13] Therefore, combined experi-

* To whom correspondence should be addressed. E-mail: carlo-adamo@enscp.fr.
[†] Chimie Paristech.
[‡] CEA Marcoule.

10.1021/jp106467p
Published on Web 09/21/2010

mental and theoretical approaches can provide valuable insight into the true nature of the vibrational bands in such difficult cases.

The theoretical modeling naturally lies within this perspective since it provides deep insight into the f elements' molecular system properties and, in particular, the nature of metal−ligand interaction. Yet, reproducing large heavy metals complexes theoretically remains challenging since they combine several drawbacks, open shells, large electron correlation, and relativistic effects. In this context, methods based on density functional theory (DFT) have been proved to be valuable tools for large heavy-metal-containing molecules, providing not only valuable information on the structure of lanthanide and actinides complexes but also details of the bonding mechanism, the role of the f orbitals, and spectroscopic features (e.g., IR and luminescence). In particular, Téllez et al. found good agreement between infrared DFT and experimental infrared spectra of diamine uranylnitrate complexes, whereas Groenewold et al. performed DFT calculations of vibrational frequencies of uranylacetone complexes within an accuracy reaching a few cm^{-1}.[14,15]

In this work, a combined experimental and theoretical analysis of metal−ligand interactions in $UO_2(NO_3)_2 \cdot 2L$ complexes, where L is *N*,*N*-dimethylformamide (DMF), *N*,*N*-dibutylformamide (DBF), or *N*,*N*-dicyclohexylformamide (DcHF), is presented. In particular, experimental and theoretical IR spectra have been carefully analyzed in order to gain some insight into the U−ligand interactions. The obtained data were then further validated by energetic and topological analysis.

2. Materials and Methods

2.1. Experimental Material. Infrared spectra were recorded with a Magna-IR 750 spectrometer (Nicolet). The neat amides were analyzed with an attenuated total internal reflectance (ATR) device, whereas the vibrational spectra of complexes $UO_2(NO_3)_2 \cdot L_2$ were recorded with a classical cell (KBr windows separated by a Teflon seal of 0.025 mm). The resolution of ATR spectra was 2 cm^{-1}. The number of scans selected was between 64 and 128.

2.2. Syntheses of Uranylnitrate Amide Complexes. DMF was a commercial product from Prolabo, and DBF and DcHF were provided by Panchim (now Pharmasynthese, Evry, France). The purity of the products was determined by elemental analyses and ^{13}C NMR and ^{1}H NMR. DcHF was a solid compound.

$UO_2(NO_3)_2 \cdot 2L$ complexes with L = DBF and DcHF were prepared by contacting 0.8 mol L^{-1} uranylnitrate hexahydrated (Fluka) with 0.4 mol L^{-1} monoamide (DBF or DcHF) diluted in *n*-dodecane (Fluka). The solution was stirred for 24 h. After filtration under vacuum, the precipitate was rinsed with *n*-hexane (Fluka) and dried in a vacuum desiccator at room temperature for 24 h.

$UO_2(NO_3)_2 \cdot 2DMF$ was prepared by dissolving uranylnitrate hexahydrate into neat DMF with a stoichiometric ratio of $UO_2(NO_3)_2$/DMF = 1/2. The precipitate was rinsed with *n*-hexane and dried in a vacuum desiccator at room temperature for 24 h.

Reference solutions, without dissociation of complexes, were the following ones: $UO_2(NO_3)_2$/DMF 0.5 M in acetone and $UO_2(NO_3)_2$/DcHF 0.17 M in toluene.

2.3. Computational Details. All geometries were fully optimized, without symmetry constraints, using the B3LYP functional[16] and the 6-31G(d,p) basis set[17,18] for light atoms (H, N, O, and C), while the quasi-relativistic effective core potential (RECP-60MWB) of the Stuttgart group[19] was used, with its valence basis set, for uranium. Such a level of theory is expected to provide accurate reproduction of structural, vibrational, and energetic features of investigated systems.[20] Furthermore, other relativistic effects beyond those included in the RECP are negligible for these kinds of complexes.[21]

Vibrational frequency calculations and thermochemical analyses were performed on the energy-minimized structures of isolated ligands and complexes. Total interaction energies were computed as $\Delta E = E_{complex} - (E_{uranylnitrate} + E_{ligands})$ and corrected for the basis set superposition error (BSSE) with the standard counterpoise model without geometry reoptimization.[22]

Electron population analyses have been performed using Natural Population Analysis (NPA).[23] For the uranium atom, two valence/Rydberg partitioning schemes have been proposed in the literature. The first one, the default partition implemented in the Gaussian code, includes 6d orbitals in the Rydberg part, while in the second, proposed by Clark and co-workers,[24] 6d orbitals are in the valence part. Following our previous experience on uranyl complexes,[25] the first one was chosen.

The electron density features were also investigated using the so-called Quantum Theory of Atoms in Molecule (QTAIM) partition scheme.[26] According to this approach, topological atoms are defined as regions in real space consisting of a bundle of electron density gradient paths attracted to a nucleus. This partition allows evaluation of atomic properties, defined as volume integrals over nonoverlapping atomic basins. In particular, the electronic population associated with an atom is simply the volume integral of the electronic charge density over the basin. Morevoer, electron density and its Laplacian where evaluated at the so-called bond critical point (BCP), a point in the space where the density gradient (but not the density itself) vanishes. The local properties at these points are in fact often used to discuss the nature of bonding.[27−29]

Solvent effects were evaluated using the Conductor-like Polarizable Continuum Model (CPCM).[30]

All the DFT calculations have been carried out using the Gaussian 03 software.[31]

3. Results and Discussion

Information on metal−ligand interactions between uranylnitrate and monoamide and IR spectra have been obtained upon energy minimization of isolated ligands, uranylnitrate, and their complexes with U(VI). To avoid a useless and tedious discussion, only a few comments will be given on the obtained structural parameters and mainly in relationship with the IR spectra. However, all of the obtained structures are reported in Tables S1 (ligands), S2 (uranylnitrate), and S3 (complexes) of the Supporting Information.

From a more computational point of view, the theoretical approach was first validated on monoamide ligands and dihydrate uranylnitrate and then applied to the uranylnitrate monoamide complexes under investigation. This order is reflected in the following.

3.1. Monoamides (Ligands). Table 1 gathers a selection of experimental and calculated vibrational frequencies of DMF, DBF, and DcHF, while the structure sketches are reported in Scheme 1. The experimental infrared spectra of pure monoamide were collected on an ATR device (see the Experimental Material section), while theoretical spectra were calculated both in the gas phase and in solution (toluene or acetone). As mentioned in the Introduction, the main IR signature of the uranyl−ligand interaction is related to the carbonyl stretching, which, therefore, will be analyzed in more detail. The C−O frequencies of the three monoamide ligands are not modified by the molecular environment. Indeed the difference of vibrational frequencies

TABLE 1: Experimental and Computed Vibrational Frequencies (cm^{-1}) for the Considered Ligands[a]

ligand	DMF	DBF	DcHF
Experiments			
$\nu(C{=}O)_{(vs)}$	1661	1665	1660
$\nu\ (C{-}N)_{(m)}$	1504	1468	1469
$\nu(NR_2)_{(w)}$	865	823	724
$\delta(O{=}C{-}N)_{(m)}$	657	689	592
Theory (solvent)			
$\nu(C{=}O)$	1732 (1665)	1728 (1661)	1727 (1660)
$\nu(C{-}N)$	1545	1485	1501
$\nu(NR_2)$	873	882	744
$\delta(O{=}C{-}N)$	659	703	555
Theory (isolated)			
$\nu(C{=}O)$	1800	1776	1775
$\nu(C{-}N)$	1553	1480	1487
$\nu(NR_2)$	879	888	745
$\delta(O{=}C{-}N)$	661	691	562

[a] In parentheses are reported empirically scaled frequencies (scaling factor equal to 0.9613; from ref 34).

SCHEME 1: Sketches of the Considered Monoamide Ligands DMF, DBF, and DcHF

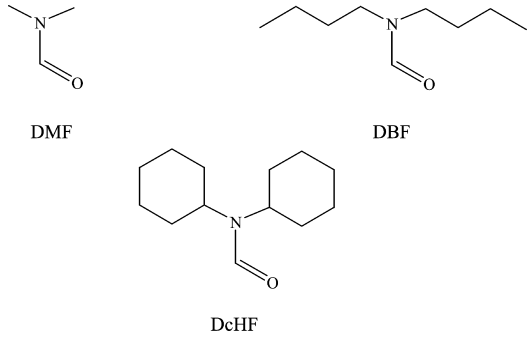

is never higher than 5 cm^{-1} for both theoretical and experimental spectra, whatever the alkyl group (methyl group for DMF, butyl group for DBF, or cyclohexyl group for DcHF). The only exception is represented by the frequency calculated in the gas phase for the DMF ligand, which shows a higher value of about 25 cm^{-1} (Table 1) with respect to the other ligands that is in line with previous work.[13] This result reflects the similar bond lengths of the carbonyl group in solution well (see Table S1, Supporting Information).

More in general, the calculated frequencies (especially at high wavenumber) are overestimated with respect to the corresponding experimental values due to the anharmonicity and to the intrinsic error of the DFT approach.[32−34] The simplest way to correct for these two combined effects is to use empirical scaling, and at the B3LYP/6-31G(d,p) level, an empirical factor of 0.9613 has been suggested.[34] Such a correction permits one to find very good (even quantitative) agreement between calculated and experimental vibrational frequencies as the carbonyl frequencies calculated in solution are 1665, 1661, and 1660 cm^{-1} for DMF, DBF, and DcHF, respectively, giving a mean deviation of 2−3 cm^{-1} with respect to experimental values. The other calculated stretching frequencies fit the experimental infrared spectra well, especially at low frequencies, where the mean deviation reaches 30−35 cm^{-1} without correction. In the following, no empirical correction will be applied unless specified in the text.

3.2. Uranylnitrate Dihydrate. The suggested speciation of uranylnitrate in concentrated nitric acid solution (54.5% in weight) is $UO_2(NO_3)_2 \cdot 2H_2O$, where the UO_2^{2+} is surrounded by four oxygens of the bidentate nitrate groups and two oxygens of the water molecules of the solvation shell.[35,36] Therefore, this species has been chosen as a reference in this first part of our study. In Figure 1, the optimized geometry of the uranylnitrate dihydrate complex in the gas phase is reported. Previous experimental and theoretical studies[14,36−38] showed that this molecular structure contains a center of symmetry with the uranium atom surrounded by eight oxygen atoms in a hexagonal bipyramidal geometry. The two uranyl oxygens occupy the axial positions, whereas two bidentate nitrate ligands and two oxygen atoms of the solvation water molecules are located in the hexagonal equatorial plane. These six equatorial oxygen atoms are approximately coplanar. As expected, the U−O axial interaction is stronger than the equatorial interaction, being characterized by shorter U−O distances ($U{-}O_{uranyl}$ = 1.77 Å). The lengths of the equatorial bonds with the water molecules ($U{-}O_w$ = 2.54 Å) and the nitrates ($U{-}O_{nitro}$ = 2.47 Å) are typical values of coordinated bonds. All of these values, including the N−O lengths of the nitrates, are in good agreement with experimental distances determined by neutron and X-ray diffraction of uranylnitrate dihydrate and trihydrate,[36,38,39] with average deviations of 0.01 Å between theory and experiment. In summary, the B3LYP approach, using the 6-31G(d,p) basis set and ECP for the U atom, leads to good evaluation of the $UO_2(NO_3)_2 \cdot 2H_2O$ structure, and consequently, it could be expected to give also a good estimation of infrared frequencies (see Table 2).

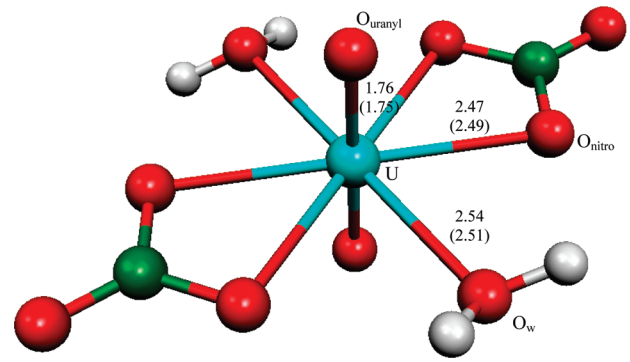

Figure 1. Optimized gas-phase structure of $UO_2(NO_3)_2 \cdot 2H_2O$.

TABLE 2: Experimental and Calculated Vibrational Frequencies (cm^{-1}) of $UO_2(NO_3)_2 \cdot 2H_2O$[a]

experimental	calculated	assignment
not observed	3899	$\nu_{as}(H{-}O{-}H)$
not observed	3782	$\nu_{s}(H{-}O{-}H)$
1605_s	1674 (1608)	$\nu(NO_3) = \nu(N{=}O)$
1532_s	1596 (1534)	$\delta(H_2O)$
1385_w		
1280_s	1307	$\nu(NO_3) = \nu_{as}(N{-}O)$
1134_w		
1027_s	1064	$\nu(NO_3) = \nu_{s}(N{-}O)$
991_w		
929_w	984	$\nu_{as}(O{-}U{-}O)$
not observed	901	$\nu_{s}(O{-}U{-}O)$
803_w	805	$_{Rocking}(NO_3)$
748_w	738	$\delta_{as}(O{-}N{-}O)$
440_w	408	$_{Rocking}(H_2O)$

[a] In parentheses are reported empirically scaled values (scaling factor equal to 0.9613; from ref 34).

The H_2O symmetric and asymmetric stretching vibrations located at 3899 and 3782 cm^{-1} are observed only in the calculated spectrum due to the low signal intensity. The band located at 1605 cm^{-1} in the experimental spectrum corresponds

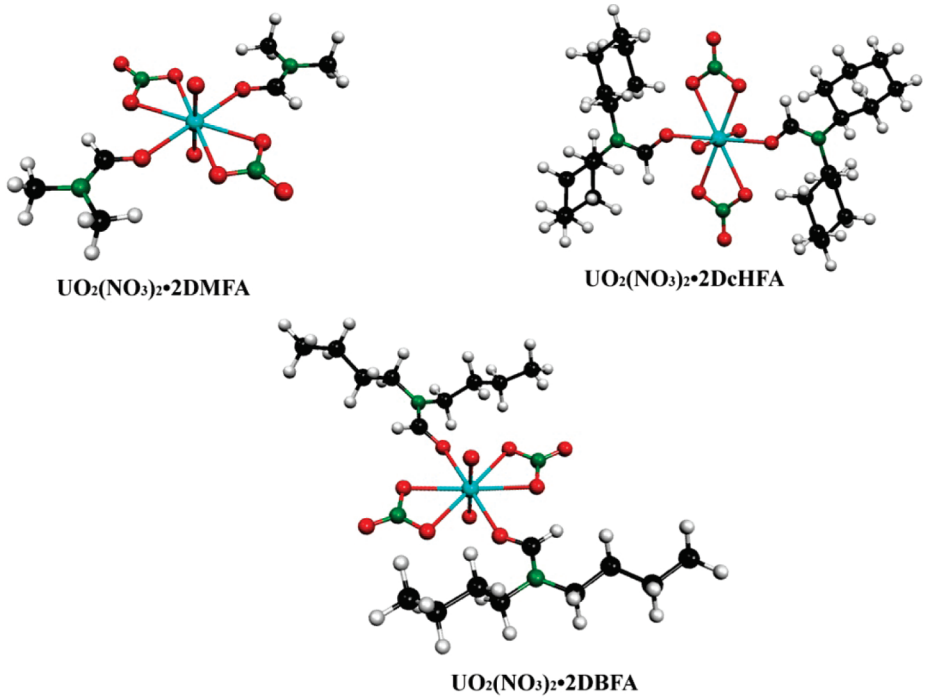

Figure 2. Optimized gas-phase structure of the investigated uranylnitrate monoamide complexes. Calculated and experimental[36] uranium−oxygen distances (Å) are also reported.

to the calculated vibrational frequency at 1674 cm^{-1}, which can be attributed to the stretching of the N═O double bond (i.e., N1−O5 in Figure 1). By correcting this calculated band by the empirical factor (see previous section),[23] the calculated vibration is in fair agreement with the experimental values with a small shift of 2−3 cm^{-1} (Table 2). The band at 1596 cm^{-1} in the calculated spectrum corresponds to the H_2O bending mode. In the experimental spectrum, this band is located at 1532 cm^{-1}. The experimental bands assigned to N1−O3 asymmetric and symmetric stretching modes (Figure 1) are observed at 1280 and 1027 cm^{-1}, and the corresponding calculated vibrational frequencies are located at 1307 and 1064 cm^{-1}. The calculated infrared spectrum exhibits two bands at 984 and 901 cm^{-1}, which correspond to asymmetric and symmetric O−U−O uranyl stretching vibrations, respectively.[40,41] The experimental spectrum shows only the asymmetric mode of this frequency (929 cm^{-1}), as reported in Table 2. The bands located at 805, 738, and 408 cm^{-1} are assigned to the NO_3 rocking mode, O−N−O asymmetric bending mode, and H_2O rocking mode, respectively (Table 2).

3.3. Nitrate Monoamide Complexes. Figure 2 displays the optimized geometries of the investigated uranylnitrate monoamide complexes. The most stable geometry of these systems corresponds to the hexagonal bipyramidal geometry, and the coordination number of uranium is 8, with the nitrate groups acting as bidentate ligands. Amide ligands act as monodentate ligands which interact with uranium through the carbonyl oxygen. Calculated bond lengths and interaction energies are reported in Table 3. The complexes are very stable, showing large interaction energies in solution, going from −233 (DMF complex) to −261 kJ/mol (DcHF). These energies are larger than those for the water−uranyl interactions in uranylnitrate dehydrate (−190 kJ mol^{-1}), that is, uranylnitrate amide complexes are more stable than uranylnitrate dehydrate.

Since all of the considered complexes have the same stoechiometry and involve similar ligands, it can be argued that the microscopic mechanism of the selective extraction process can be directly related to the formation of more stable complexes due to a stronger electronic interaction, all other factors (e.g., entropy) being similar within the series.

TABLE 3: Calculated Bond Length (Å) and Interaction Energies (kJ/mol) in the Considered Uranium Complexes

	ΔE	$U-O_{uranyl}$	C═O	$U-O_{ligand}$	N═O	N−O
$UO_2(NO_3)_2$•2DMF						
gas phase	−233	1.768	1.243	2.459	1.211	1.283
solution	−233	1.771	1.249	2.431	1.213	1.281
$UO_2(NO_3)_2$•2DBF						
gas phase	−256	1.765	1.251	2.437	1.213	1.283
solution	−254	1.774	1.255	2.410	1.215	1.281
$UO_2(NO_3)_2$•2DcHF						
gas phase	−254	1.769	1.251	2.434	1.212	1.283
solution	−261	1.779	1.256	2.418	1.214	1.281

The different interaction strengths are reflected in slight differences for the bond lengths of $U-O_{uranyl}$ and carbonyls (C═O) and their distance with uranium ($U-O_{ligand}$; see Table 3). Indeed, the CO length increases in going from DMF to DcHF complexes (+0.008 Å), while the $U-O_{ligand}$ decreases (−0.013 Å). Thus, the energetic behavior matches the geometrical changes well. The NO bonds are not affected by complex formation as they are almost similar in all of the investigated compounds.

In Table 4 are collected the main computed and experimental vibrational frequencies of the uranium complexes. As already discussed for the isolated ligands, there is an overall good agreement between experimental and theoretical frequencies, with deviations ranging (on average) between 20 (ν_{ONO}) and 50 cm^{-1}, this larger deviation for the highest wave numbers (ν_{NO}). A similar precision can be extrapolated for the $\nu(O_{lig}UO)$, which cannot be assigned directly from experimental infrared spectra. More interesting, the difference between the CO stretching frequency in complexes and that in the isolated ligand, which is considered as a probe of the metal−ligand interaction, is reproduced within a few cm^{-1} (see Table 3).

In Figure 3 is reported the experimental spectrum of the DcHF complex, together with the theoretical transitions. These latter

TABLE 4: Calculated (Gas-Phase and Solution) and Experimental Vibration Frequencies (cm^{-1}) for All of the Considered Uranium Complexes[a]

	ν_{as}(C−O)	$\Delta\nu$(CO)	ν_{as}(O−U−O)$_{ura}$	ν_{as}(O−U−O)$_{lig}$	ν(N=O)	ν_{as}(N−O)
			$UO_2(NO_3)_2$·2DMF			
Theory						
gas phase	1720	−80	976	686	1651	1335
solution (acetone)	1704 (1638)	−28	954	684	1611 (1549)	1329
Experiment						
pure	1648	−13	929		1524	1283
solution (acetone)	1645	−16	939		1524	1268 (?)
			$UO_2(NO_3)_2$·2DBF			
Theory						
gas phase	1708	−68	973	713	1637	1336
solution (toluene)	1688 (1622)	−40	953	713	1610 (1548)	1332
Experiment						
pure	1628	−37	940	−	1522	1278
			$UO_2(NO_3)_2$·2DcHF			
Theory						
gas phase	1690	−85	973	755	1643	1338
solution	1679 (1614)	−48	941	751	1617 (1557)	1333
Experiment						
toluene	1619	−41	936	−	1531	1276
pure	1618	−42	940		1519	1279

[a] In parentheses are reported empirically scaled values (scaling factor equal to 0.9613; from ref 34).

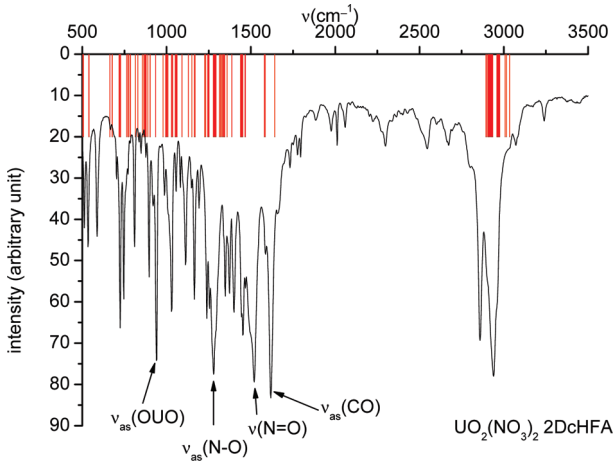

Figure 3. Experimental IR spectra (black line) and theoretical vibrational frequencies (red) for the solid $UO_2(NO_3)_2$·2DcHF complex.

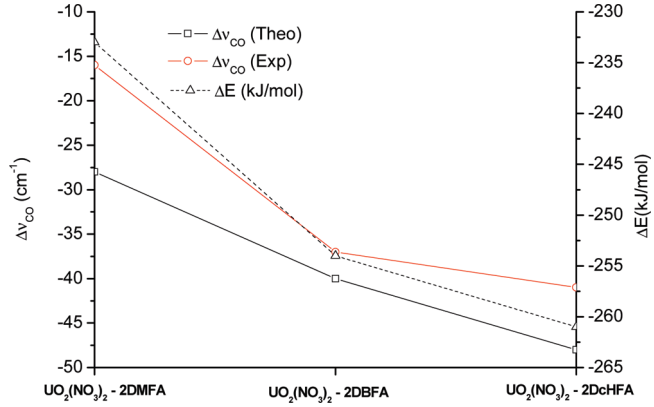

Figure 4. Correlation between the experimental and theoretical shifts of the carbonyl stretching frequency ($\Delta\nu_{CO}$) with the interaction energy along the uranyl complexes series.

are represented as sticks since, due to the relatively small basis set considered, a poor representation of the intensities is expected.[42] The quantitative agreement between theoretical and experimental data clearly appears from this figure, with all of the theoretical transitions well grouped under the most intense experimental bands. A similar overall behavior is found also for the other two ligands, whose spectra are reported in Figures S1 and S2 of the Supporting Information.

Figure 4 shows experimental and theoretical frequency shifts of the carbonyls ($\Delta\nu$(CO)) in the solid phase versus the interaction energy along the uranyl complex series (Table 4 indicates that the position of the frequency ν(CO) was not affected by the diluent). This figure exhibits good agreement between experimental and theoretical $\Delta\nu$(CO) values, the two data sets being only slightly shifted. This slight overestimation may be explained by the solvent effect model as theoretical calculations were performed in neat toluene or neat acetone whereas experimental infrared spectra were recorded for a 0.5 mol L^{-1} uranylnitrate monoamide complex in toluene for $UO_2(NO_3)_2$·2DcHF or a 0.17 mol L^{-1} uranylnitrate monoamide complexe acetone for $UO_2(NO_3)_2$·2DMF. In fact, the presence of the uranylnitrate monoamide complex is responsible for a decrease of the dielectric constant, which was not taken into account in the DFT calculations where the dielectric constant of pure diluent (toluene or acetone) was considered. The $\Delta\nu$(CO) index is a good indicator for estimating the metal ligand interaction as it is proportional to the BSSE corrected interaction energy (Figure 4).

More interesting, it must be emphasized that both theoretical and experimental shifts are negative, that is, a decrease of the vibrational frequency is observed in going from the bare to the complexed ligands. It could be argued, therefore, that no specific orbital interaction (like in the Dewar−Chatt−Duncanson model[43]) is at work between uranium and formamide ligands. This interaction could be, instead, electrostatic in nature.

Some insight into the electronic structure of the investigated complexes has been obtained by calculating atomic charges with the QTAIM and NPA approaches for the three uranylamide complexes. From the QTAIM charges of Table 5, it appears

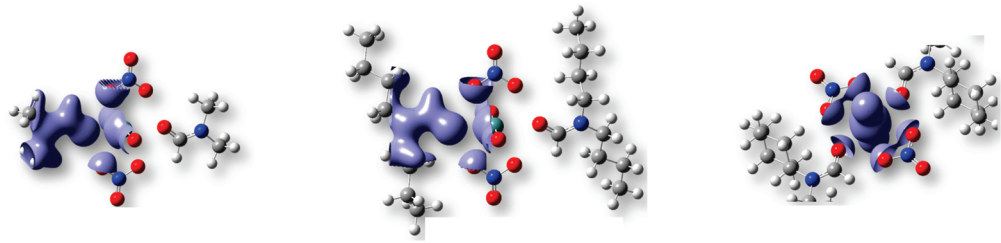

Figure 5. Graphical representation of the electron density surface at the U−O critical point, for all complexes.

TABLE 5: Quantum Theory of Atoms in Molecules (QTAIM) and Natural Population Analysis (NPA) Charges (|e⁻|)

	AIM							NPA						
	C	O_{ligand}	N_{ligand}	H_{ligand}	ligands	U	UO_2	C	O_{ligand}	N_{ligand}	H_{ligand}	ligands	U	UO_2
$UO_2(NO_3)_2$·2DMF	1.492	−1.217	−1.179	0.129	0.208	3.078	1.316	0.558	−0.719	−0.417	0.138	0.286	2.862	1.109
$UO_2(NO_3)_2$·2DBF	1.472	−1.212	−1.166	0.122	0.228	3.068	1.304	0.550	−0.727	−0.381	0.144	0.302	2.856	1.094
$UO_2(NO_3)_2$·2DcHF	1.463	−1.214	−1.120	0.120	0.229	3.061	1.301	0.553	−0.728	−0.382	0.200	0.297	2.854	1.096

that there is a slight decrease of the uranyl charge (formally +2 |e⁻|) in going from DMF to DcHF, from 1.32 to 1.30 |e⁻|. Consequently, the charge on the amide ligands increases from 0.21 to 0.23 |e⁻|, while that on nitrates is constant (about 0.87 |e⁻|). This latter result suggests that nitrate ligands do not modulate the interaction energy along the amine series.

Moreover, the close charge values observed for all of the ligands suggest that the uranyl−amide interaction is mainly ruled by electrostatic interactions. Indeed, the increase of stability observed from DMF to DcHF complexes is directly linked to the degree of polarization of the ligands in interaction with the metal cation. The small increase of intermolecular charge transfer is just a consequence of the huge charge redistribution but does not participate in the increase of stability. The most stable ligand ($UO_2(NO_3)_2$·2DcHF) has a higher degree of polarization and an especially higher positive charge delocalization in the outer part of the ligand molecule than $UO_2(NO_3)_2$·2DMF, which is characterized by a more concentrated positive charge close to the uranyl ion (UO_2^{2+}). The intramolecular charge polarization effect is evident looking at the atomic charge variation in going from DBF to DcHF complexes (N_{ligand} and C), which does not match with the trend observed for the overall ligand charge (constant).

The NPA analysis gives the same trend, albeit with a small modulation. Indeed, in this case, the average charge on uranyl is 1.1 |e⁻|, and that on the ligands is 0.3 |e⁻|, thus giving the same charge on nitrates (about −0.8 |e⁻|). This concordance between NPA and QTAIM values, together with those obtained on other actinides and uranyl complexes,[25,29] confirms the choice of the standard NBO partition scheme.

In order to further confirm the electrostatic nature of the metal−ligand interaction mechanism and to support experimental analysis, topological studies of the electron density have also been performed. The value of the electronic density and its Laplacian at the bond critical point (r_c) are reported in Table S4 (Supporting Information), while Figure 5 shows the electronic density for all complexes. The low value of electronic density at metal−ligand critical points (i.e., $\rho(r_c) \approx 0.05$ au, Table S4 (Supporting Information) and Figure 5) and the strong local depletion ($\nabla\rho(r_c)c > 0$) confirm a pure electrostatic interaction between the metal and oxygen atoms of the ligands. For instance, the electronic density at the bond critical point in Figure 5c is close to that of a compound such as NaF, whose bonding is purely electrostatic.[44] The same trend can be found between the metal and nitrate anions (Table S4, Supporting Information).

4. Conclusion

Vibrational frequencies of DMF, DBF, DcHF, and corresponding uranylnitrate monoamide complexes have been calculated with good accuracy by DFT calculations.

A careful QTAIM analysis has been performed to characterize electron-charge transfers and metal−ligand interactions. It has been found that the difference of vibrational frequency between the CO stretching frequency in the complex and the CO stretching frequency in the isolated ligand is a good indicator of the uranium−monoamide interaction. The related stretching variations, obtained in going from the free to complexed ligand, are not due to a back-donating charge transfer from the metal to the ligand but are a consequence of a deep redistibution of the electron density in the ligand itself. This redistibution, induced by the strong electrostatic interaction with the metal, is proportional to the degree of polarizability of the ligand, from DMF to DcHF.

Acknowledgment. The authors thank the Agence Nationale pour la Recherche (ANR) for the financial support of the project AMPLI.

Supporting Information Available: Optimized structure of ligands, uranylnitrate, and complexes; experimental and theoretical IR spectra; and the electronic density and its Laplacian at the bond critical point. This material is available free of charge via the Internet at http://pubs.acs.org.

References and Notes

(1) Musikas, C.; Schulz, W. W.; Liljenzin, J. O. *Solvent Extraction in Nuclear Science and Technology, in Solvent Extraction Principles and Practice*; Marcel Dekker: New York, 2004; p 507.
(2) Moyer, B. *Ion Exchange and Solvent Extraction, A Series of Advances*; CRC Press: Boca Raton, FL, 2009; Vol 19.
(3) Moore, R. L. USAEC Report AECD; U.S. Army Environmental Command: 1951; p 3196.
(4) Siddall, T. H. *J. Phys. Chem.* **1960**, *64*, 1863.
(5) (a) Gasparini, G. M.; Grossi, G. *Solv. Extr. Ion Exchange* **1986**, *4*, 1233D. (b) Musikas, C. *Sep. Sci. Technol.* **1988**, *23*, 1211.
(6) Ruikar, P. B.; Nagar, M. S.; Subramanian, M. S. *J. Radioanal. Nucl. Chem.* **1991**, *2*, 473.

(7) Gupta, K. K.; Manchanda, V. K.; Subramanian, M. S.; Singh, R. K. *Sep. Sci. Technol.* **2000**, *35*, 1603.

(8) Rabbe, C.; Sella, C.; Madic, C.; Godard, A. *Solvent Extr. Ion Exch.* **1999**, *17*, 87.

(9) Rabbe, C.; Madic, C.; Godard, A. Solv. *Solvent Extr. Ion Exch.* **1999**, *16*, 1091.

(10) Condamines, N.; Turq, P.; Musikas, C. *Solvent Extr. Ion Exch.* **1993**, *11*, 187.

(11) Clement, O.; Rapko, B. M.; Hay, B. P. *Coord. Chem. Rev.* **1998**, *170*, 203.

(12) Hay, B. P.; Clement, O.; Sandrone, G.; Dixon, D. A. *Inorg. Chem.* **1998**, *37*, 5887.

(13) Zhou, X.; Krauser, J. A.; Tate, D. R.; VanBuren, A. S.; Clark, J. A.; Moody, P. R.; Liu, R. *J. Phys. Chem.* **1996**, *100*, 16822.

(14) Téllez Soto, C. A.; Carauta, A. N. M.; Carneiro, J. W. de M. *Spectrochim. Acta, Part A* **2008**, *71*, 1140.

(15) Groenewold, G. S.; Gianotto, A. K.; Cossel, K. C.; Van Stipdonk, M. J.; Moore, D. T.; Polfer, N.; Oomens, J.; de Jong, W. A.; Visscher, L. *J. Am. Chem. Soc.* **2006**, *107*, 4802.

(16) Becke, A. D. *J. Chem. Phys.* **1993**, *98*, 5648.

(17) Hariharan, P. C.; Pople, J. A. *Theor. Chim. Acta* **1973**, *28*, 213.

(18) Francl, M. M.; Petro, W. J.; Hehre, W. J.; Binkley, J. S.; Gordon, M. S.; DeFrees, D. J.; Pople, J. A. *J. Chem. Phys.* **1982**, *77*, 3654.

(19) (a) Kuechle, W.; Dolg, M.; Stoll, H.; Preuss, H. *J. Chem. Phys.* **1994**, *100*, 7535. (b) Cao, X.; Dolg, M.; Stoll, H. *J. Chem. Phys.* **2003**, *118*, 487.

(20) (a) Michelini, M. C.; Russo, N.; Sicilia, E. *Angew. Chem., Int. Ed.* **2006**, *45*, 1095. (b) Michelini, M. C.; Russo, N.; Sicilia, E. *J. Am. Chem. Soc.* **2007**, *129*, 4229.

(21) Vetere, V.; Maldivi, P.; Roos, B. O.; Adamo, C. *J. Phys. Chem. A* **2009**, *113*, 1476.

(22) Boys, S. F.; Bernardi, F. *Mol. Phys.* **1970**, *19*, 553.

(23) (a) Reed, A. E.; Weinstock, R. B.; Weinhold, F. *J. Chem. Phys.* **1985**, *83*, 735. (b) Foster, J. P.; Weinhold, F. *J. Am. Chem. Soc.* **1980**, *102*, 7211. (c) Reed, A. E.; Curtiss, L. A.; Weinhold, F. *Chem. Rev.* **1988**, *88*, 899.

(24) Clark, A. E.; Sonnenberg, J. L.; Hay, P. J.; Martin, R. L. *J. Chem. Phys.* **2004**, *121*, 2563.

(25) Boulet, B.; Joubert, L.; Cote, G.; Bouvier-Capely, C.; Cossonnet, C.; Adamo, C. *Inorg. Chem.* **2008**, *47*, 7983.

(26) Bader, R. W. F. *Atoms in Molecules. A Quantum Theory*; Oxford University Press: Oxford, U.K., 1990.

(27) Bader, R. F. W.; Essén, H. *J. Chem. Phys.* **1984**, *80*, 1943.

(28) Tognetti, V.; Joubert, L.; Adamo, C. *J. Chem. Phys.* **2010**, *132*, 211101.

(29) Petit, L.; Joubert, L.; Maldivi, P.; Adamo, C. *J. Am. Chem. Soc.* **2006**, *128*, 2190.

(30) (a) Tomasi, J.; Persico, M. *Chem. Rev.* **1994**, *94*, 2027. (b) Barone, V.; Cossi, M. *J. Phys. Chem. A* **1998**, *102*, 1995.

(31) Frisch, M. J.; Trucks, G. W.; Schlegel, H. B.; Scuseria, G. E.; Robb, M. A.; Cheeseman, J. R.; Montgomery, J. A., Jr.; Vreven, T.; Kudin, K. N.; Burant, J. C.; Millam, J. M.; Iyengar, S. S.; Tomasi, J.; Barone, V.; Mennucci, B.; Cossi, M.; Scalmani, G.; Rega, N.; Petersson, G. A.; Nakatsuji, H.; Hada, M.; Ehara, M.; Toyota, K.; Fukuda, R.; Hasegawa, J.; Ishida, M.; Nakajima, T.; Honda, Y.; Kitao, O.; Nakai, H.; Li, X.; Knox, J. E.; Hratchian, H. P.; Cross, J. B.; Adamo, C.; Jaramillo, J.; Gomperts, R.; Stratmann, R. E.; Cammi, R.; Pomelli, C.; Ochterski, J.; Ayala, P. Y.; Morokuma, K.; Hase, W. L.; Salvador, P.; Dannenberg, J. J.; Zakrzewski, V. G.; Dapprich, S.; Daniels, A. D.; Strain, M. C.; Farkas, O.; Malick, D. K.; Rabuck, A. D.; Raghavachari, K.; Foresman, J. B.; Ortiz, J. V.; Cui, Q.; Baboul, A. G.; Clifford, S.; Cioslowski, J.; Stefanov, B. B.; Liu, G.; Liashenko, A.; Piskorz, P.; Komaromi, I.; Martin, R. L.; Fox, D. J.; Keith, T.; Al-Laham, M. A.; Peng, C. Y.; Nanayakkara, A.; Challacombe, M.; Gill, P. M. W.; Johnson, B.; Chen, W.; Wong, M. W.; Gonzalez, C.; Pople, J. A. *Gaussian 03*; Gaussian, Inc.: Pittsburgh, PA, 2003.

(32) (a) Bienati, M.; Adamo, C.; Barone, V. *Chem. Phys. Lett.* **1999**, *311*, 69. (b) Andersson, M. P.; Uvdal, P. *J. Phys. Chem. A* **2005**, *109*, 2937.

(33) (a) Chermette, H. *Coord. Chem. Rev.* **1998**, *178*, 699. (b) Wong, M. W. *Chem. Phys. Lett.* **1996**, *256*, 391.

(34) Scott, A. P.; Radom, L. *J. Phys. Chem.* **1996**, *100*, 16502.

(35) Taylor, J. C.; Mueller, M. H. *Acta Crystallogr.* **1965**, *19*, 536.

(36) Dalley, N. K.; Mueller, M. H.; Simonsen, S. H. *Inorg. Chem.* **1971**, *10*, 323.

(37) Kannan, S.; Deb, S. B.; Gamare, J. S.; Drew, M. G. B. *Polyhedron* **2008**, *27*, 2557.

(38) Hirata, M.; Monjyushiro, H.; Sekine, R.; Onoe, J.; Nakamatsu, V.; Mukoyama, T.; Adachi, H.; Takeuchi, K. *J. Electron. Spectrosc.* **1997**, *83*, 59.

(39) Hughes, K. A.; Burns, P. C. *Acta Crystallogr.* **2003**, *C59*, i7.

(40) Topping, L. *Spectrochim. Acta* **1965**, *21*, 1743.

(41) Ohwada, K. *Spectrochim. Acta* **1979**, *35A*, 1283.

(42) Halls, M. D.; Schlegel, H. B. *J. Chem. Phys.* **1998**, *109*, 10587.

(43) (a) Dewar, M. *Bull. Soc. Chim. Fr.* **1951**, *18*, C79. (b) Chatt, J.; Duncanson, L. A. *J. Chem. Soc.* **1953**, 2939.

(44) Bader, R. F. W.; Johnson, S.; Tang, T. H.; Popelier, P. L. A. *J. Phys. Chem.* **1996**, *100*, 15398.

JP106467P